that H_2O accounts for 80% of the total gas production [D. Krankowsky *et al.*, *Nature* **321**, 326 (1986)].
9. The solar wind conditions in the models were obtained from WIND satellite data (http://web.mit.edu/afs/athena/orgls/space/www.html), interpolated for 27.0 March UT since WIND was in the magnetosheath. The solar wind parameters used in the simulation were: speed = 470 km/s, number density = 6 cm^{-3}, solar wind temperature = 8.8×10^4 K, magnetic field components $B_x = 4.5$ nT, $B_y = -2.0$ nT, $B_z = 0$ nT.
10. R. A. Phaneuf, I. Alvarez, F. W. Meyer, D. H. Crandall, *Phys. Rev. A* **26**, 1892 (1982).
11. H. Tawara, *At. Data Nucl. Data Tables* **22**, 491 (1978).
12. L. Haser, *Bull. Acad. R. Belg. Classes Sci. Ser. 5* **43**, 740 (1957).
13. M. R. Combi, *Icarus* **123**, 207 (1996).
14. R. E. Olson, *J. Phys. B At. Mol. Opt. Phys.* **13**, 483 (1980).
15. R. E. Olson and D. R. Schultz, *Phys. Scripta T* **28**, 71 (1989).
16. The expected count rates for the ROSAT instruments have been calculated for a geocentric distance of 0.127 AU using the energy-dependent effective area of the instruments as published in the ROSAT user's manual (http://ftp.rosat.mpe-garching/mpg.de/). The degradation of the WFC sensitivity with time after launch has been taken into account.
17. The solar wind composition and charge state distribution of ions vary considerably with time [for example, R. von Steiger, S. P. Christon, G. Gloeckler, F. M. Ipavich, *Astrophys. J.* **389**, 791 (1992)]. CXE cross sections have errors of 20 to 30%. The measured gas production rate and solar wind parameters have errors of 10 to 20%. Other ions, such as N, Si, and F, have not yet been included.
18. The O/H ratios are from S. J. Bame, J. R. Asbridge, W. C. Feldman, M. D. Montgomery, and P. D. Kearney [*Sol. Phys.* **43**, 463 (1975)]. The C/O ratios are from (23). The Ne/O ratios are from J. Geiss, R. von Steiger, G. Gloeckler, and A. B. Galvin [*Eos* **75** (no. 16), 278 (1994)].
19. C. Lisse *et al.*, http://www.astro.umd.edu/~lisse/rosat.html.
20. R. Bingham, J. M. Dawson, V. D. Shapiro, D. A. Mendis, B. J. Kellett, *Science* **275**, 49 (1996).
21. V. A. Krasnopolsky, *Bull. Am. Astron. Soc.* **28**, 1095 (1996).
22. T. G. Northrop, C. M. Lisse, M. J. Mumma, M. D. Desch, *Icarus*, in press.
23. P. Bochsler, J. Geiss, S. Kunz, *Sol. Phys.* **103**, 177 (1986).
24. R. L. Kelly and L. J. Palumbo, *Atomic and Ionic Emission Lines Below 2000 Angstroms* (Naval Research Laboratory, Washington, DC, 1973).
25. This work was supported by NASA under grants NAGW-1907, NAGW-1366, and NCCS5-146 and by NSF under grants AS7-9618795 and ATM-9318181. R.M.H. acknowledges partial support by the Swiss National Science Foundation. We thank T. E. Cravens for helpful discussions.

4 March 1997; accepted 17 April 1997

A Proficient Enzyme Revisited: The Predicted Mechanism for Orotidine Monophosphate Decarboxylase

Jeehiun K. Lee and K. N. Houk

A mechanism is proposed to explain the activity of orotidine 5′-monophosphate decarboxylase (ODCase). This enzyme is the one of the most proficient known, with a catalytic proficiency $(k_{cat}/K_m)/k_{non} = 10^{23}$ M^{-1}. Quantum mechanical calculations predict a mechanism involving a stabilized carbene intermediate, which represents a previously unrecognized mode of enzymatic activity for ODCase. The proposed mechanism involves proton transfer from a weak acid ($pK_a = 7$, where K_a is the acid constant) concerted with decarboxylation, in a nonpolar enzyme environment. Such a mechanism makes possible different approaches to the design of ODCase inhibitors. Furthermore, the prediction that general acid catalysis may only be effective in low dielectric media is of general significance for understanding the activity of many enzymes.

The decarboxylation of orotidine 5′-monophosphate (OMP) (Fig. 1, **1a**; all bold numbers here refer to labeled structures in Fig. 1) to form uridine 5′-monophosphate (UMP, **2a**) by orotidine 5′-monophosphate decarboxylase (ODCase) is an essential step in nucleic acid biosynthesis (*1*). In bacteria and fungi, ODCase exists alone as a separate protein, whereas in mammals the ODCase activity is part of a bifunctional protein, UMP synthase (*2*). The conversion of **1** to **2** is also biomechanistically unique, in that all other biochemical decarboxylations involve stabilization of the carbanion intermediate by delocalization of the electron pair into a π orbital (*3*, *4*). For the decarboxylation of **1**, however, no such stabilization is present; a nonconjugated carbanion is formed. ODCase is one of the most proficient enzymes known (*1*). Proficiency is the second-order rate constant for the enzymatic reaction divided by the nonenzymatic rate constant $[(k_{cat}/K_m/k_{non})]$. For ODCase, the proficiencey is 2.0×10^{23} M^{-1}. The catalytic efficiency (k_{cat}/K_M) of ODCase, as with many enzymes, is nearly diffusion-controlled (*1*); it is the excruciating slowness of the uncatalyzed decarboxylation ($k_{non} = 2.8 \times 10^{-16}$ s^{-1}) that produces the high proficiency.

The mechanism by which ODCase effects the efficient decarboxylation has long been a subject of interest among chemists and biochemists but remains unknown (*1*, *5*). The lack of any detectable cofactors or metal ions makes this mechanistic problem even more intriguing (*6*–*9*). Although no crystal structure of ODCase exists (*10*, *11*), it has been shown that 6-azauridylate (**3a**) and barbituric acid ribonucleotide (**4a**) are particularly prodigious inhibitors of yeast ODCase [inhibition constant $(K_I) = 5.1 \times 10^{-7}$ and 8.8×10^{-12} M, respectively] (*5*, *8*). Studies by Jones *et al.* of the enzyme mechanism indicate that Lys^{93} is important for catalysis but not for binding (*12*). In addition, the ratio of the maximal catalytic rate V_{max} to K_M of ODCase is pH-dependent, with a maximum at pH 7; this result has been interpreted to indicate that the enzyme possesses a catalytic group that has a pK_a of ~7 (*7*, *12*). Recently, catalytic antibodies have been developed to catalyze the decarboxylation of orotate (*9*, *13*).

Various mechanistic hypotheses have been proposed to explain the enormous rate enhancement by ODCase. Silverman *et al.* suggested a covalent mechanism involving nucleophilic attack at C-5, but this was subsequently shown by ^{13}C and D isotope effects to be unlikely (*6*, *7*, *14*). Beak *et al.* examined the decarboxylation of 1,3-dimethylorotic acid in sulfolane and proposed that decarboxylation occurred via zwitterion (**5**) (*5*). The fast (4×10^8 acceleration over the parent reaction) decarboxylation of betaine (**6**) led the authors to propose that the enzyme might effect catalysis by favoring formation of zwitterion (**5**). This mechanism has long been widely accepted (*6*–*9*, *15*). The protonation of the weakly basic orotate to form the zwitterion, however, seems unlikely.

An enzyme as proficient as ODCase is expected to be unusually "sensitive to . . . reversible inhibitors [that are] designed to resemble the [transition structure]" (*1*). The biological and medicinal importance of this reaction is clear: As a key biosynthetic step, the decarboxylation is a natural target for antitumor agents and genetic diseases such as orotic aciduria. Knowledge of the transition structure facilitates inhibitor design; herein, calculations are used to predict a transition state for this biologically and medicinally important reaction.

The energetics of the decarboxylation were explored by full optimizations of geometries and reaction paths along the decarboxylation reaction coordinate with the use of restricted Hartree-Fock (RHF) calculations with the 6-31+G* basis set. Energetics were obtained by single-point sec-

Department of Chemistry and Biochemistry, University of California, Los Angeles, CA 90095, USA.

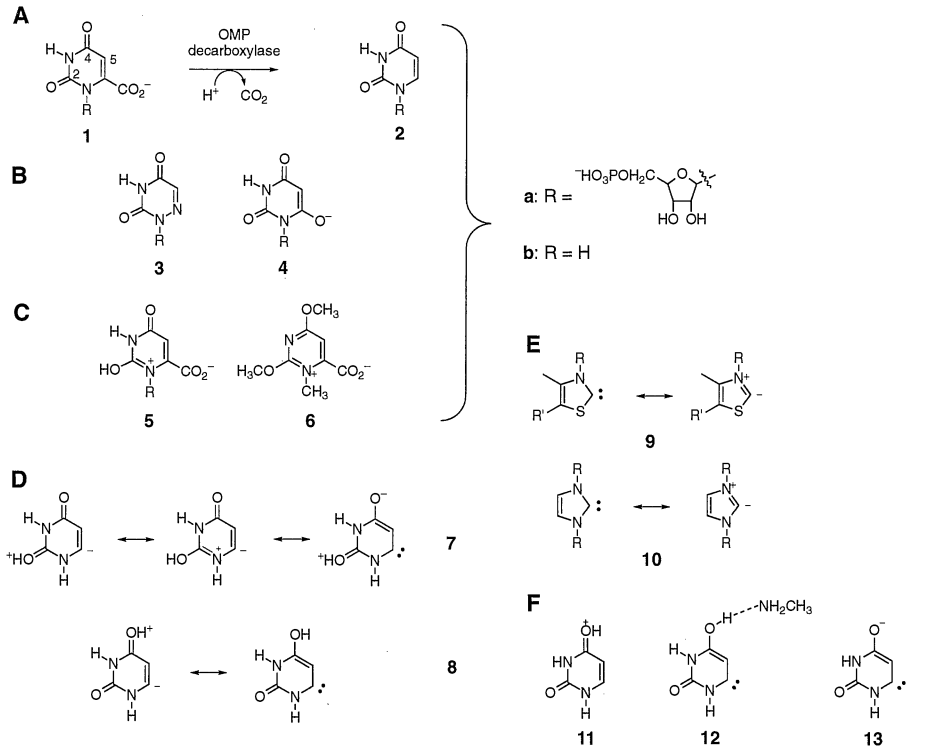

Fig. 1. (**A**) The decarboxylation of OMP. (**B**) Inhibitors of ODCase. (**C**) Proposed intermediate zwitterion (**5**) and model compound (**6**). (**D**) Zwitterion resulting from 2-protonation of orotate (**7**) and zwitterion resulting from 4-protonation of orotate (**8**). (**E**) Known stabilized carbenes: thiazolium ylide of thiamine (**9**) and stabilized carbene (**10**). (**F**) 4-protonated uracil (**11**), proposed model transition state (**12**), and anionic carbene (**13**) resulting from decarboxylation of orotate.

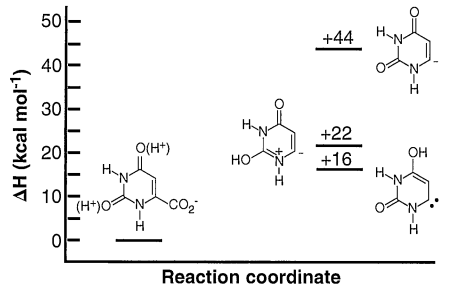

Fig. 2. Calculated $\Delta H^{\ddagger}$ values (MP2/6-31+G*//RHF/6-31+G*) for the decarboxylation of orotate, 2-protonated orotate, and 4-protonated orotate.

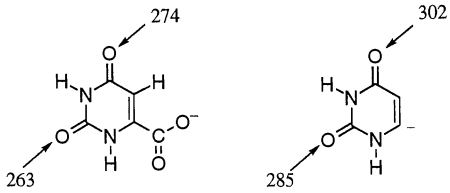

Fig. 3. Calculated gas-phase proton affinities (in kilocalories per mole) of orotate (left) and deprotonated uracil (right) (MP2/6-31+G*//RHF/6-31+G*).

ond-order Møller-Plasset (MP2) energy calculations on the RHF geometries (*16*). The parent reaction of **1b** is endothermic in the gas phase (activation enthalpy, $\Delta H^{\ddagger}$ = +43.9 kcal mol^{-1}), and there is no barrier to recombination of CO_2 with the carbanion (*17*). We next examined the decarboxylation of the 2-protonated orotate **5b**, which was proposed by Beak to be an intermediate for the catalyzed reaction. The decarboxylation of 2-protonated orotate is endothermic by only +21.6 kcal mol^{-1} at the MP2/6-31+G* level. These gas-phase results are in accord with the Beak mechanism: decarboxylation of 2-protonated orotate **5b** is 22 kcal mol^{-1} less endothermic than the decarboxylation of orotate itself (**1b**).

Product **7**, formed from decarboxylation of 2-protonated orotate, can be represented by several resonance structures; one of these is a carbene with separated charges (Fig. 1D). For better stability, we envisioned a neutral carbene that did not have separated charges (*18*). Such a structure (**8**, Fig. 1D) is obtainable by protonation of orotate at the 4-oxygen and decarboxylation. Indeed, the reaction to form **8** is a very favorable process: The decarboxylation of 4-protonated orotate has an extraordinarily low barrier—only +15.5 kcal mol^{-1}.

The $\Delta H^{\ddagger}$ values calculated for these three reactions (decarboxylation of orotate, 2-protonated orotate, and 4-protonated orotate) are shown in Fig. 2. The entropy change associated with decarboxylation is between 23 and 27 entropy units for all the reactions at 298 K. The $\Delta H^{\ddagger}$ for the decarboxylation of orotate at 298 K is calculated to be 44.5 kcal mol^{-1}, and the free energy of activation $\Delta G^{\ddagger}$ is 36.4 kcal mol^{-1}. These gas-phase values are not sensitive to solvation and can be compared favorably to the experimental values of 44.4 and 38.5, respectively (*1*). Protonation at the 2-position accelerates the reaction, as predicted by Beak ($\Delta G^{\ddagger}$ = 14.0 kcal mol^{-1}, $\Delta H^{\ddagger}$ = 21.6 kcal mol^{-1}), but protonation at the 4-position drops the barrier for decarboxylation by an additional 6 kcal mol^{-1} ($\Delta G^{\ddagger}$ = 8.0 kcal mol^{-1}, $\Delta H^{\ddagger}$ = 15.5 kcal mol^{-1}).

Density functional methods verify the energetics of orotate and 4-protonated orotate decarboxylation. With Becke3LYP/6-31+G* calculations (*16*), the $\Delta G^{\ddagger}$ at 298 K for orotate decarboxylation is 36.7 kcal mol^{-1}, which is consistent with our MP2/6-31+G*//RHF/6-31+G* and experimental values. The 4-protonated orotate decarboxylates with a $\Delta G^{\ddagger}$ of 9.0 kcal mol^{-1}, which is also consistent with our MP2 values. Thus, quantum mechanical methods lead to a prediction that protonation at O-4 lowers the activation free energy by 28 kcal mol^{-1}, leading to a stabilized carbene intermediate.

Carbenes are usually considered to be reactive intermediates of only fleeting existence; nevertheless, the carbene **8** is likely to be the intermediate responsible for ODCase's extraordinary proficiency. The possibility of a stabilized carbene such as **8** has biological precedence in the form of thiamine pyrophosphate. The thiazolium ylide (**9**) of thiamine is formed quite easily ($pK_a \sim 19$ to 20) and is also nucleophilic; such carbenes gain unusual stability because of ylide resonance (*19*, *20*). Stabilized carbenes (**10**) have also been successfully synthesized, crystallized, and characterized by Arduengo and co-workers, who have shown that some derivatives are "true carbenes with negligible ylidic character" (*21*).

Another fundamental mechanistic question involves the nature of the proton transfer to O-4. Does protonation occur first, followed by decarboxylation, or is proton transfer concerted with decarboxylation? The predicted gas-phase acidities of each position of orotate and deprotonated uracil are shown in Fig. 3. Two primary points can be drawn from these values: First, the 4-oxygen position is always more basic than the 2 position. Experimentally, uracil is known to be protonated at the 4-oxygen, not the 2-oxygen (*22*). Second, decarboxylation increases the basicity of the oxygen by a substantial amount (by 28 kcal mol^{-1} for the 4 position). In the gas phase, a viable base such as $MeNH_3^+$ (pro-

ton affinity = 214 kcal mol^{-1}) (*23*) easily and exothermically transfers a proton to both species shown in Fig. 3. However, in water, protonation of either reactant or product is unlikely; the pK_a of 4-protonated uracil (**11**) is about 0.5 (*22*) and that of orotate should be only slightly higher (~1.5) (*24*). The pK_a of the catalytic group in ODCase has been experimentally measured at 7 (*7, 12*). The pK_a of lysine in aqueous solution is 10.5 (*25*); presumably, the dielectric of the relatively nonpolar cavity and neighboring side chains in the enzyme active site drops this value to 7. The pK_a of protonated orotate might be raised somewhat above ~1.5 in the nonpolar enzyme active site, but protonation of the starting material orotate is still highly unlikely to occur by proton transfer from a catalytic group with pK_a = 7. Indeed, equilibrium protonation would occur at the carboxylate oxygen, a process that would shut down decarboxylation entirely. How can the enzyme manage to deliver a proton to the 4-oxygen? Proton transfer concerted with decarboxylation can take advantage of the large increase in basicity during the departure of CO_2. This form of general acid catalysis demonstrates Jencks' "libido rule," which postulates that "concerted general acid-base catalysis of complex reactions . . . can occur only (a) at sites that undergo a large change of pK in the course of the reaction, and (b) when . . . the pK of the catalyst is intermediate between the initial and final pK values of the substrate site" (*26*).

This mechanism requires a particular environment, which must be provided by the enzyme active site. For example, concerted proton transfer to O-4 will not occur in an aqueous environment, because lysine is insufficiently acidic. However, our computational investigations show that in an appropriate environment that is likely to be present in the enzyme, the proton transfer to the 4-oxygen concerted with decarboxylation becomes very favorable.

The magnitudes of dielectric constants of enzyme active sites have been the subject of extensive discussions, with predicted values ranging from 2 to 40 (*27–29*). Recent theoretical work predicts that protein interiors possess low dielectric constants in the range of 3 to 6 (*30*). We explored the effect of placing the reacting species within solvent cavities of four different dielectric constants; the calculated values of $\Delta H^{\ddagger}$ for the decarboxylation of bare orotate (uncatalyzed model) and the reaction of orotate with methyl ammonium to form carbene (**12**) plus CO_2 (catalyzed model) in these various cavities are summarized in Table 1 (*31*). Calculations on the uncatalyzed process show that the barrier to orotate decarboxylation is not very sensitive to solvent, as would be expected for a reaction with anionic starting material and product. However, the decarboxylation concerted with proton transfer from the ammonium group varies greatly in exothermicity depending on the environment. In the gas phase, the reaction is exothermic by a huge amount (61.9 kcal mol^{-1}). In a medium of dielectric constant (ε) equal to 4, the $\Delta H^{\ddagger}$ jumps to +17.6 kcal mol^{-1}. At a value of ε = 10, the $\Delta H^{\ddagger}$ rises to +33.7 kcal mol^{-1} as the increasingly polar solvent selectively stabilizes the ionic starting materials relative to the less polar products. In water (ε = 78.54) the reaction is significantly endothermic, at +43.2 kcal mol^{-1}. The data in the third row of Table 1 provide the activation energy change upon 4-protonation in four different dielectric environments. In water, there is no advantage to 4-protonation at all. At the other extreme, the 4-protonation would be favored by an enormous amount in the gas phase (105.8 kcal mol^{-1}). Our calculations therefore predict that only a low dielectric constant allows energetics that are ideal for catalysis. Using an ε = 4 to mimic the enzyme's hydrophobic interior (*30*), we find that the difference in activation energy calculated for the parent reaction in water and our proposed catalytic mechanism in dielectric 4 is 24.8 kcal mol^{-1}, essentially identical to that found experimentally (Fig. 4). Even assuming some differences associated with entropy changes and binding interactions, the calculated value still compares favorably to the experimental value. Thus, we predict that the mechanism by which OMP decarboxylates in the ODCase active site is via a stabilized carbene intermediate that results from concerted proton transfer to the 4 position; this proton transfer, though yielding a carbene, results in the rate acceleration of 10^{17}. To complete the catalytic cycle, we envision the protonation of the carbene in Fig. 4 by water, which would allow for formation of bicarbonate and for proton transfer from protonated uracil back to the catalytic lysine.

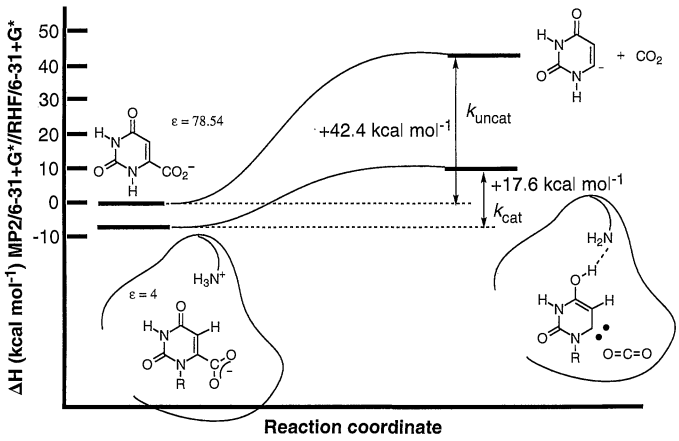

Fig. 4. Energy diagram showing barrier to decarboxylation for orotate in water and for orotate plus $CH_3NH_3^+$ in a dielectric of 4, which is our working model for the ODCase catalyzed reaction.

Table 1. Energies of reaction of orotate (**1b**) plus $CH_3NH_3^+$ to form a carbene-methylamine complex (**12**) plus CO_2 (enzyme-catalyzed reaction model) in cavities with various dielectric constants (ε). The energies are calculated at MP2/6-31+G*//RHF/6-31+G*. The energies of the uncatalyzed process (**1b** → **13** + CO_2) and the differences are given for comparison.

Reaction	$\Delta H^{\ddagger}$ (kcal mol^{-1})			
	(ε = 1)	(ε = 4)	(ε = 10)	(ε = 78.54)
Uncatalyzed	+43.9	+41.5	+42.5	+42.4
Catalyzed	−61.9	+17.6	+33.7	+43.2
Uncatalyzed − catalyzed	+105.8	+23.9	+8.8	−0.8

The potent inhibition of ODCase by barbiturate 5′-monophosphate (BMP, **4a**) can be explained by its similarity to the decarboxylation transition state and the fact that it should be protonated by the catalytic acid of ODCase. The pK_a of BMP in water is only about 4.5 (*8*), but in the enzyme active site, by analogy to our previous discussion, we expect the pK_a to rise to about 8. Therefore, proton transfer from the catalytic group to BMP is favorable and viable. Furthermore, our calculations show that anionic carbene (**13**) and barbiturate (**4b**) have similar proton affinities in the gas phase [302 kcal mol^{-1} for carbene (**13**) versus 304 kcal mol^{-1} for barbiturate (**4b**)]. The perfect transition state analog would match the shape and electrostatic potential of the carbene-like transition state and have a pK_a greater than 7 for protonation in the area occupied by the 4-oxygen.

The mechanism proposed here requires an environment of low dielectric (similar in polarity to ether or chloroform) and will not be observed in aqueous solution. Therefore,

the active site of ODCase must provide two features: a low dielectric interior to allow for pK_a tuning so that the catalytic proton transfer to O-4 can occur, and a perfectly placed lysine to effect that proton transfer to O-4, concerted with decarboxylation.

REFERENCES AND NOTES

1. A. Radzicka and R. Wolfenden, *Science* **267**, 90 (1995).
2. R. W. McClard, M. J. Black, L. R. Livingstone, M. E. Jones, *Biochemistry* **19**, 4699 (1980).
3. T. C. Bruice and S. Benkovic, in *Bioorganic Mechanisms* (Benjamin, New York, 1966), vol. 2, pp. 188–194.
4. M. L. Bender, in *Mechanisms of Homogeneous Catalysis from Protons to Proteins* (Wiley-Interscience, New York, 1971), pp. 165–175 and 586–594.
5. P. Beak and B. Siegel, *J. Am. Chem. Soc.* **98**, 3601 (1976).
6. S. A. Acheson, J. B. Bell, M. E. Jones, R. Wolfenden, *Biochemistry* **29**, 3198 (1990).
7. J. A. Smiley, P. Paneth, M. H. O'Leary, J. B. Bell, M. E. Jones, *ibid.* **30**, 6216 (1991).
8. H. L. Levine, R. S. Brody, F. H. Westheimer, *ibid.* **19**, 4993 (1980).
9. J. A. Smiley and S. J. Benkovic, *Proc. Natl. Acad. Sci. U.S.A.* **91**, 8319 (1994).
10. J. B. Bell, M. E. Jones, C. W. J. Carter, *Proteins* **9**, 143 (1991).
11. Attempts to obtain the crystal structure of ODCase are underway (C. Carter, personal communication).
12. J. A. Smiley and M. E. Jones, *Biochemistry* **31**, 12162 (1992).
13. J. A. Smiley and S. J. Benkovic, *J. Am. Chem. Soc.* **117**, 3877 (1995).
14. R. B. Silverman and M. P. Groziak, *ibid.* **104**, 6434 (1982).
15. K. Shostak and M. E. Jones, *Biochemistry* **31**, 12155 (1992).
16. Gaussian 94, revision B.3 (M. J. Frisch *et al.*, Gaussian, Inc., Pittsburgh, PA, 1995). RHF, MP2, and basis sets are described by W. J. Hehre, L. Radom, P. v. R. Schleyer, and J. A. Pople [*Ab Initio Molecular Orbital Theory* (Wiley, New York, 1986)]. Density functional theory (Becke3LYP) is described by W. Kohn, A. D. Becke, and R. G. Parr [*J. Phys. Chem.* **100**, 12974 (1996)].
17. Unless otherwise specified, the calculated $\Delta H^{\ddagger}$ is for 0 K.
18. D. Lavorato *et al.*, *J. Am. Chem. Soc.* **118**, 11898 (1996), and references therein.
19. R. Kluger, *Chem. Rev.* **87**, 863 (1987).
20. D. Kern *et al.*, *Science* **275**, 67 (1997).
21. A. J. Arduengo III *et al.*, *J. Am. Chem. Soc.* **116**, 6812 (1994), and references therein.
22. R. Wagner and W. von Philipsborn, *Helv. Chim. Acta* **53**, 299 (1970).
23. S. G. Lias *et al.*, *J. Phys. Chem. Ref. Data* **17**, (suppl. no. 1) (1988).
24. Using the difference in the pK_a of acetic acid and malonic acid to estimate the effect of a CO_2^- group, we estimate the pK_a of protonated orotate to be ~1.5.
25. J. A. Dean, in *Lange's Handbook of Chemistry* (McGraw-Hill, San Francisco, CA, 1992), pp. 8.19–8.71.
26. W. P. Jencks, *J. Am. Chem. Soc.* **94**, 4731 (1972).
27. M. K. Gilson and B. H. Honig, *Biopolymers* **25**, 2097 (1986).
28. G. King, F. S. Lee, A. Warshel, *J. Chem. Phys.* **95**, 4366 (1991).
29. A. Warshel and J. Åqvist, *Annu. Rev. Biophys. Biophys. Chem.* **20**, 267 (1991).
30. T. Simonson and C. L. Brooks III, *J. Am. Chem. Soc.* **118**, 8452 (1996).
31. Solvation was modeled with the SCI-PCM method, available in Gaussian 94 (*16*). Solvation energies were obtained by calculating RHF/6-31+G* energies in solvent of a given dielectric and comparing that value to the gas-phase energy. These solvation energies were then used to correct MP2/6-31+G* energies to obtain $\Delta H^{\ddagger}$ values in solution.

32. We are grateful to NSF and NIH (postdoctoral fellowship to J.K.L.) for financial support of this work and to the UCLA Office of Academic Computing and the National Center for Supercomputing Applications for computational resources.

16 December 1996; accepted 19 March 1997

An Elicitor of Plant Volatiles from Beet Armyworm Oral Secretion

H. T. Alborn, T. C. J. Turlings,* T. H. Jones, G. Stenhagen, J. H. Loughrin,† J. H. Tumlinson‡

The compound *N*-(17-hydroxylinolenoyl)-L-glutamine (named here volicitin) was isolated from oral secretions of beet armyworm caterpillars. When applied to damaged leaves of corn seedlings, volicitin induces the seedlings to emit volatile compounds that attract parasitic wasps, natural enemies of the caterpillars. Mechanical damage of the leaves, without application of this compound, did not trigger release of the same blend of volatiles. Volicitin is a key component in a chain of chemical signals and biochemical processes that regulate tritrophic interactions among plants, insect herbivores, and natural enemies of the herbivores.

The intriguing defensive reaction of plants, whereby plant volatiles induced by insect herbivore injury attract natural enemies of the herbivores, is triggered when a substance in the oral secretion of the insect herbivores contacts damaged plant tissue. We have isolated, identified, and synthesized *N*-(17-hydroxylinolenoyl)-L-glutamine (Fig. 1), which we have named volicitin, from the oral secretion of beet armyworm (BAW) (*Spodoptera exigua* Hübner) caterpillars. Synthesized and natural volicitin induce corn (*Zea mays* L.) seedlings to release the same blend of volatile terpenoids and indole released when they are damaged by caterpillar feeding (*1*). This blend of volatile compounds attracts females of the parasitic wasp *Cotesia marginiventris*, natural enemies of BAW caterpillars, to the damaged corn plants (*2*).

The similarity of the structure of the insect-produced elicitor with the structures of the precursors of eicosanoids and prostaglandins involved in signaling in insects and other animals (*3*) and the components of the octadecanoid signaling pathway in plants (Fig. 1) (*4*) indicates a link between these two systems. The octadecanoid pathway is involved in induction of biosynthesis and release of volatiles in response to insect herbivore feeding (*5*, *6*).

We collected oral secretions (about 5 μl per caterpillar) by squeezing third to fifth instar BAW caterpillars that had been fed on corn seedlings, causing them to regurgitate (*1*). Biological activity was determined by collection and capillary gas chromatographic (GC) analysis (*7*) of volatiles from corn seedlings treated with oral secretion or subsequent fractions thereof (*8*).

The crude oral secretion was acidified, centrifuged, and filtered to remove proteins and solids (*9*). When the filtered oral secretion was fractionated on a reversed phase solid-phase extraction cartridge (*9*), the total activity of the original crude secretion eluted from the reversed phase cartridge with 50% CH_3CN in H_2O, indicating a molecule of medium polarity.

We further purified the active material from solid-phase extraction by a series of reversed-phase high-performance liquid chromatography (rpHPLC) fractionations using three sets of conditions (*10*). Only one active component, detected by monitoring ultraviolet (UV) absorption at 200 nm and with no absorption above 220 nm, eluted from the final column, and its biological activity was equivalent to that of the original crude oral secretion. The active material was extracted into CH_2Cl_2 from an acidified (pH 3) aqueous solution but not from an aqueous solution at pH 8 (*11*). All biological activity could be extracted from the organic phase back into pH 8 buffer, indicating lipid character and an acidic functional group. A CH_2Cl_2 solution of the active material was also fractionated on a

H. T. Alborn, T. C. J. Turlings, J. H. Loughrin, J. H. Tumlinson, Center for Medical, Agricultural, and Veterinary Entomology, United States Department of Agriculture, Agricultural Research Service, 1700 Southwest 23rd Drive, Gainesville, FL 32608, USA.
T. H. Jones, Department of Chemistry, Virginia Military Institute, Lexington, VA 24450, USA.
G. Stenhagen, Department of Organic Chemistry, Chalmers University of Technology, S-412 96 Göteborg, Sweden.

*Present address: University of Neuchatel, Institute of Zoology, CH-2007 Neuchatel, Switzerland.
†Present address: Community Research Service, Kentucky State University, Frankfort, KY 40601, USA.
‡To whom correspondence should be addressed. E-mail: tumlnsn@nervm.nerdc.ufl.edu